Available online at www.sciencedirect.com
ScienceDirect
Icarus 188 (2007) 139–153
ICARUS
www.elsevier.com/locate/icarus

Ammonium sulfate on Titan: Possible origin and role in cryovolcanism

A.D. Fortes *, P.M. Grindrod, S.K. Trickett, L. Vočadlo

Department of Earth Sciences, University College London, Gower Street, London, WC1E 6BT, UK

Received 9 June 2006; revised 1 November 2006

Available online 19 December 2006

Abstract

We model the chemical evolution of Titan, wherein primordial NH_3 reacts with sulfate-rich brines leached from the silicate core during its hydration. The resulting differentiated body consists of a serpentinite core overlain by a high-pressure ice VI mantle, a liquid layer of aqueous ammonium sulfate, and a heterogeneous shell of methane clathrate, low-pressure ice Ih and solid ammonium sulfate. Cooling of the subsurface ocean results in underplating of the outer shell with ice Ih; this gravitationally unstable system can produce compositional plumes as ice Ih ascends buoyantly. Ice plumes may aid in advection of melt pockets through the shell and, in combination with surface topography, provide the necessary hydraulic pressure gradients to drive such melts to the surface. Moreover, contact between the magma and wall rock (methane clathrate) will allow some methane to dissolve in the magma, as well as eroding fragments of wall rock that can be transported as xenoliths. Upon rising to the clathrate decomposition depth (∼2 MPa, or 1700 m), the entrained xenoliths will break down to ice + methane gas, powering highly explosive eruptions with lava fountains up to several kilometers high. Hence we predict that Titan is being resurfaced by cryoclastic ash consisting of ice and ammonium sulfate (or its tetrahydrate), providing an abundance of sedimentary grains, a potential source of bedload for fluvial transport and erosion, and of sand-sized material for aeolian transport and dune-building. The infrared reflectance spectrum of ammonium sulfate makes it a plausible candidate for the 5 μm-bright material on Titan's surface.

Keywords: Titan; Volcanism; Interiors; Ices

1. Introduction

The favored paradigm regarding the internal structure of Titan consists of a rocky core overlain by an ice-rich mantle bearing a deep underground ocean of aqueous ammonia (e.g., Grasset and Sotin, 1996; Grasset et al., 2000; Tobie et al., 2005). Speculation regarding the possibility of cryovolcanic activity on Titan (e.g., Lorenz, 1996), which is now apparently being borne out, has focused upon aqueous ammonia (or ammonia + methanol) as the likely cryomagma (cf., Kargel, 1992; Mitchell et al., 2006). Measurements of the viscosity of ammonia–water mixtures have been used to infer that cryovolcanoes and flows on Titan will resemble terrestrial basaltic analogues (Kargel et al., 1991). Indeed, the best candidate volcanic edifice, Ganesa Macula and its associated flow deposits, bears comparison with basaltic deposits elsewhere in the Solar System (Lopes et al., 2007). However, there are question marks over (i) the initial quantity of ammonia accreted by Titan (if any), and (ii) the stability of ammonia in aqueous solution during the differentiation process. Since these two questions are absolutely central to understanding the evolution of Titan's interior we begin, in Sections 1.1 and 1.2, by discussing the issues in more detail before, in Section 2, addressing a possible solution—a new structural model of Titan's interior. Titan's surface composition and geology—principally relating to igneous activity—provides a window into the moon's interior, and thus a test of the structural model: Section 3 therefore focuses on modeling the mechanisms and styles of possible cryovolcanism on Titan.

1.1. The abundance of NH_3 in Titan

Initial chemical models of the saturnian subnebula (Lewis and Prinn, 1980; Prinn and Fegley, 1981) suggested a relatively large inventory of ammonia in Titan's interior, 18 ± 6 wt% NH_3 (Hunten et al., 1984). A proportion of this is thought to

* Corresponding author.
E-mail address: andrew.fortes@ucl.ac.uk (A.D. Fortes).

0019-1035/$ – see front matter
doi:10.1016/j.icarus.2006.11.002

have been converted to N_2 by photolysis, radiolysis and thermolytic destruction in meteorite impacts (Atreya et al., 1978; Lunine and Stevenson, 1987; McKay et al., 1988), this being the ultimate source of Titan's N_2 atmosphere, although Zahnle et al. (1992) showed that the present atmosphere could have been sourced from a veneer of post-accretion cometary volatiles. Mousis et al. (2002) presented a new turbulent evolutionary model which indicates that the yield of CH_4 and NH_3 would actually have been insignificant even in the warmer, dense saturnian subnebula, concluding that the materials which went to form the saturnian satellites probably contained only small quantities of primordial CH_4 and NH_3 from the Primitive Solar Nebula (PSN); i.e., $CO/CH_4 \approx 5$ and $N_2/NH_3 \approx 3$. This being the case, the mass fraction of NH_3 in Titan's mantle would have been just 1.6 wt% NH_3, a value which is essentially identical to that found in comets (e.g., Meier et al., 1994; Bird et al., 1997; Lara et al., 2004). The turbulent evolutionary model does not account for the catalytic effect of iron grains in the PSN and the possibility that other grain surface reactions could yield $N_2/NH_3 < 1$ (e.g., Ruffle and Herbst, 2000). For example, taking $N_2/NH_3 = 0.1$ yields a mass fraction of ammonia in Titan's mantle of 10.9 wt% NH_3. However, the oxidation state of nitrogen in the PSN will have mirrored the oxidation state of carbon, and reduced carbon in the form of methane certainly does occur in Titan's atmosphere. Since the spectroscopically observed ratio CH_4/CO in Titan's atmosphere is ≈1000 (López-Valverde et al., 2005), then one may deduce that Titan did indeed accrete a large volume of CH_4 from the saturnian subnebula. Nonetheless, it is not necessarily true that this translates into a reducing, ammonia-rich, subnebula: Sekine et al. (2005) modeled the catalytic production of CH_4 and its accretion into Titan in an otherwise oxidized saturnian subnebula where all of the nitrogen was present as N_2. There exists the possibility that all of the observed methane was produced in Titan's interior by serpentinization reactions at the core-mantle boundary (e.g., Zolotov et al., 2005), although it is not obvious that this mechanism could produce methane with the essentially protosolar value of $^{12}C/^{13}C$ observed today; the measured ratio is 82.3 (Niemann et al., 2005), and the solar value is 89.9 (Anders and Grevesse, 1989). Similarly, CH_4 production by a population of methanogens (Fortes, 2000) would almost certainly result in isotopically lighter methane than is observed.

The last recourse to estimating the oxidation state of nitrogen in Titan is the Ar/N ratio, since both Ar and N_2 would be accreted in similar proportions by gas trapping (either in amorphous ice or as clathrate hydrates), whereas NH_3 is accreted as a stoichiometric hydrate. Accretion of nitrogen as N_2 produces a larger Ar/N ratio than accretion as NH_3 (Owen, 2000). In fact the only argon detected in Titan's atmosphere is radiogenic ^{40}Ar rather than primordial ^{36}Ar (Niemann et al., 2005), which might be taken to support the notion that Titan accreted NH_3 and not N_2. However, the non-detection of noble gases in Titan's atmosphere may be due to the formation of 'air' clathrates on the surface (Fortes and Stofan, 2005; Osegovic and Max, 2005).

It has also been argued that Titan is a captured body which accreted directly from the PSN (Prentice, 1984), having an oxidized bulk composition (i.e., N_2 and CO) and—perhaps like Pluto and Triton—having acquired a CH_4/N_2 atmosphere from a population of Kuiper belt planetesimals (cf., Zahnle et al., 1992).

1.2. The stability of NH_3 in Titan

The present paradigm overlooks the chemical interaction between the 'icy' fraction of Titan and the 'rocky' component during differentiation. In the absence of ammonia, one might expect the silicates to become hydrated, and the soluble fraction of the chondritic material to pass into solution. This scenario was investigated theoretically by Kargel (1991) for the icy Galilean moons, and led to the prediction that oxidized sulfur (primarily in the form of $MgSO_4$) would be dissolved in the volatile fraction, crystallizing $MgSO_4$–Na_2SO_4 hydrates in the mantle and producing cryovolcanic brine flows at the surface (see also Kargel et al., 2000; Spaun and Head, 2001; Zolotov and Shock, 2001). Subsequent data from the Near Infrared Mapping Spectrometer (NIMS) aboard the Galileo spacecraft, and from the Keck telescope, appears to support the hypothesis that sulfates are present on the surface of Europa (McCord et al., 1999; Dalton, 2003; Dalton et al., 2005; Spencer et al., 2006) and Ganymede (McCord et al., 2001), and that these are associated with fractures and melt-through zones where cryovolcanic liquids have been erupted (Orlando et al., 2005). Experimental study of the high P–T hydration of chondritic rocks (Scott et al., 2002) also confirms that sulfur is expressed as sulfate at pressures up to 1.5 GPa: higher pressures and temperatures favor the formation of sulfides. Chemical thermodynamic modeling of the water–rock interaction has led to an alternative scenario for Europa (McKinnon and Zolensky, 2003) in which the subsurface ocean is reduced—although the excess hydrogen may be lost to space (Zolotov and Shock, 2003)—and contains virtually no sulfate at all. Many of the arguments in that debate are particular to Europa; for example, one of the impediments to long-term stability of a sulfate ocean is intimate contact with silicate igneous materials on the ocean floor, a situation that does not occur in larger bodies—such as Ganymede and Titan—where a thick ice layer separates the ocean from the silicate core. In this paper, we accept a priori that primitive sulfates are (i) present, and (ii) leached into solution.

Aqueous solutions of ammonia in proto-Titan will also have been able to interact chemically with silicates (Engel et al., 1994) and with other substances in solution, such as sulfates. The NH_4^+ ion behaves like an alkali metal, and readily substitutes for these in silicates and other compounds. Given the reactivity of ammonia, and its possible low abundance, we must question whether any free ammonia can survive, particularly in the presence of concentrated brines, and therefore whether the eruption of ammonia–water liquids at the surface is likely. Kargel (1992) briefly discussed the interaction between aqueous ammonia and brine solutions, and now, in Section 2, we consider the logical conclusion of amalgamating a sulfate-

bearing Galilean moon model (Kargel, 1991) with an ammonia- and methane-bearing Titan model.

2. A new internal structure for Titan

2.1. Chemical and structural evolution

Our proto-Titan consists of a 'rock' component, for which we use carbonaceous chondritic material as an analogue, and a 'volatile' component, which consists of water ice, ammonia hydrate, and methane clathrate; we take the molar ratio NH_3:CH_4 = 1, which is comparable to the value found in comets (see Iro et al., 2003, and references therein). During the differentiation process, the interior of Titan becomes sufficiently hot, due to accretional heating and short-lived radioisotopes (e.g., Castillo et al., 2006) to melt the ice and hydrate component, leading to complete degassing of methane clathrate: the rock fraction yields up its water soluble fraction (assumed to be 10 wt% of the core mass, and dominated by $MgSO_4$), and is subsequently serpentinized, taking up as much as 13 wt% H_2O to form the hydrous silicate mineral antigorite. Fig. 1 illustrates the stability of antigorite with respect to mixtures of anhydrous minerals (forsterite and clinoenstatite) co-existing with water bracketing the P, T conditions in Titan's core; thermal dehydration occurs if the core temperature exceeds 850–900 K (see Wunder and Schreyer, 1997; Angel et al., 2001; Hilairet et al., 2006).

Magnesium sulfate in aqueous solution reacts with ammonia to form soluble ammonium sulfate (the mineral mascagnite), and insoluble magnesium hydroxide (the mineral brucite):

$$MgSO_4 + 2NH_3 + 2H_2O \leftrightarrow (NH_4)_2SO_4 + Mg(OH)_2. \quad (1)$$

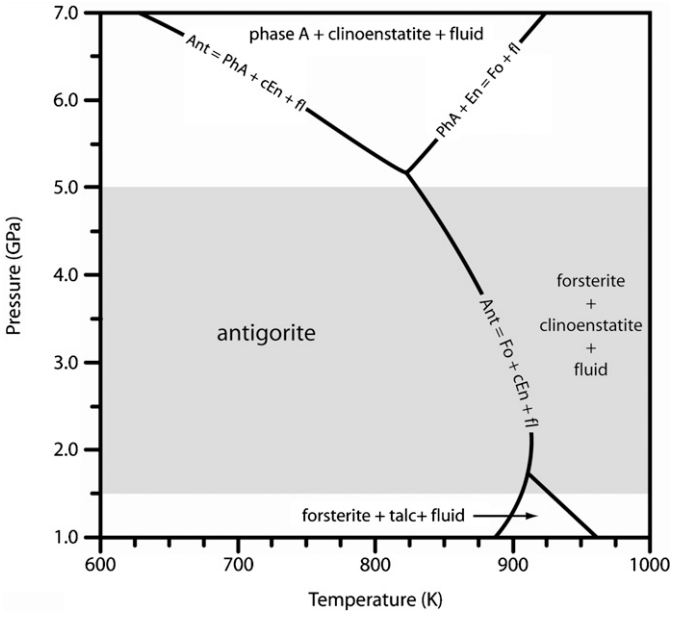

Fig. 1. Phase boundaries in the water-saturated magnesium silicate system showing the stability of the serpentine mineral, antigorite, relative to the anhydrous minerals, olivine and clinopyroxene. The shaded zone shows the range of pressures expected in Titan's core. For the indicated reactions, Ant = antigorite; PhA = hydrous silicate phase A; cEn = clinoenstatite; Fo = forsterite; and fl = fluid. Redrawn, with alterations, after Hilairet et al. (2006).

The thermodynamics of this reaction at elevated pressures are not known, and we assume for the sake of simplicity that it can and does proceed to completion. Brucite precipitates out, forming a layer on top of the hydrated rocky core where it probably is stable; dehydroxylation of brucite in contact with a concentrated brine, to periclase + fluid, requires temperatures of ~900 K (Bai and Koster van Groos, 1998). We deliberately ignore the role of 'other' minor sulfates (such as Na_2SO_4 and K_2SO_4), which will form soluble hydroxides and thus remain in the aqueous phase, providing a sink for much of the Moon's ^{40}K.

Methane is initially accreted as clathrate, and subsequently degassed, forming a hot dense atmosphere, along with nitrogen formed by the dissociation of ammonia. The underlying liquid layer, which at this stage consists of a weak solution of ammonium sulfate (ca. 15 wt%), is saturated with methane throughout its column depth. The pressure at the base of the liquid layer (order 1 GPa) is considerably higher than any existing solubility measurements for methane in pure water or concentrated brines. Based on the measured solubility of methane in brines at pressures up to 0.25 GPa (O'Sullivan and Smith, 1970; Handa, 1990; Levkam and Bishnoi, 1997), we apply a mean value of 1.5 mol% for the bulk solubility of methane in the entire ocean. Cooling of the ocean–atmosphere system eventually leads to the formation of a solid methane clathrate crust at the ocean surface. Once this has begun, dissolved methane in the underlying liquid is driven down the combined solubility/thermal gradient to crystallize clathrate at the base of the crust, causing it to thicken. This likely occurs by the direct nucleation of clathrate from dissolved gas in the liquid phase. However, where the liquid phase becomes supersaturated and methane gas is exsolved, then clathrates will grow at the gas–liquid interface of these bubbles as they (i) rise through the ocean column (Rehder et al., 2002; Ohmura et al., 2004; Sauter et al., 2006; Greinert et al., 2006), and/or (ii) are mechanically trapped in a crystal mush at the base of the crust (cf., Haeckel et al., 2004; Torres et al., 2004). The crystallization of methane clathrate excludes dissolved salts, increasing the salinity of the residual liquid (Ussler and Paull, 2001), further lowering the solubility of methane and promoting the thickening of the crust. In addition, macro-porous clathrate grains will carry pockets of ammonium sulfate solution upwards and incorporate them into the outer shell, where they will ultimately solidify to ice + ammonium sulfate (and/or ammonium sulfate tetrahydrate; see Xu et al., 1998). During the formation and growth of the shell, we would also expect major melt-throughs due to thermal plumes and impact events, as well as local thermally-, compositionally-, or tidally-driven volcanism, to emplace large volumes of aqueous ammonium sulfate at the surface and within the crust. We assume in our calculation of the thickness and bulk density of the crust that it incorporates 25 wt% of the ocean; terrestrial sea ice, for example, often contains up to 40% liquid in brine pockets and grain-boundary fluid (Perovich and Gow, 1996). Underneath the clathrate shell, continued cooling of the aqueous ammonium sulfate ocean will precipitate high-pressure ice VI, which sinks and accumulates on the ocean floor, driving the composition of the residual liquid towards the binary eutectic

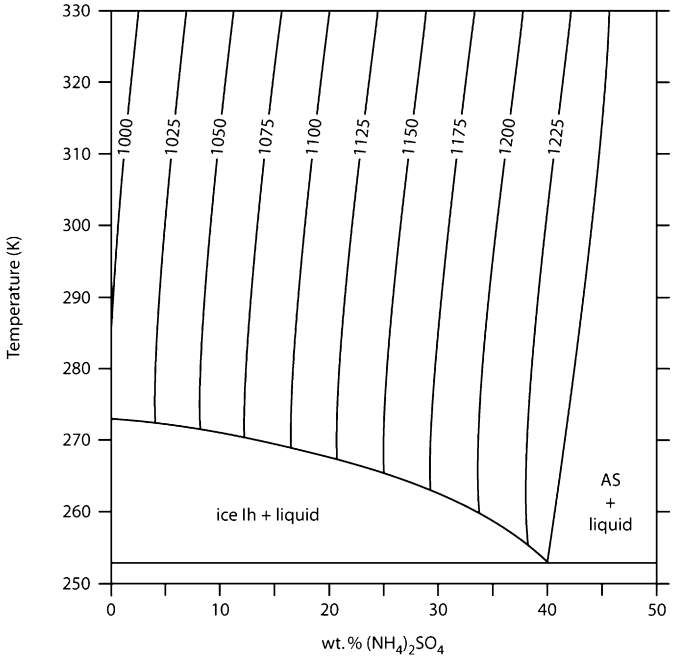

Fig. 2. The water-rich half of the binary $(NH_4)_2SO_4$–H_2O system at atmospheric pressure, redrawn after Xu et al. (1998). The liquidus field is contoured to show the density (kg m^{-3}) of the aqueous solution (calculated from coefficients in Novotný and Söhnel, 1988).

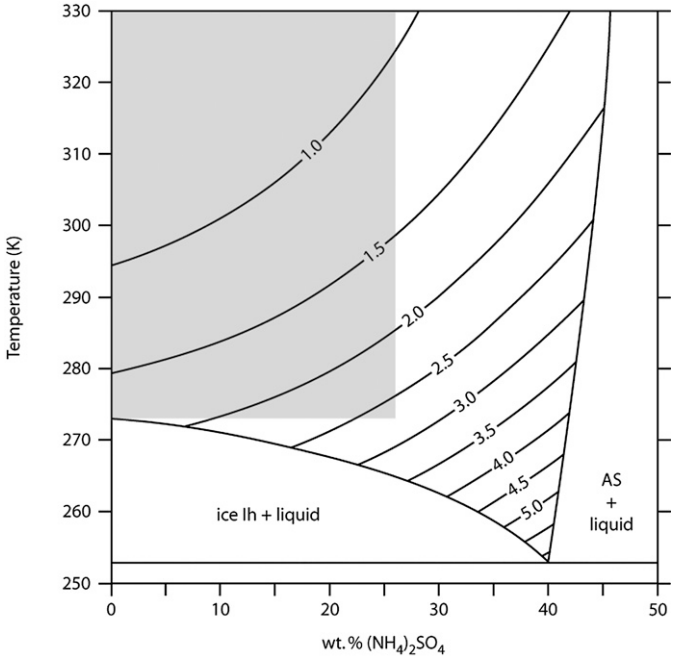

Fig. 3. The water-rich half of the binary $(NH_4)_2SO_4$–H_2O system at atmospheric pressure, redrawn after Xu et al. (1998). The liquidus field is contoured to show the viscosity (mPa s) of the aqueous solution, derived by fitting a polynomial function to data in Sprung (1876) over the range 0–25.5 wt%, 0–60 °C (this region, with good data coverage, is shaded grey) and to data in the CRC Handbook (Lide, 2005) over the range 0—saturation at 25 °C.

at 40.0 wt% $(NH_4)_2SO_4$, 253.8 K (N.B., this is the *ambient pressure* eutectic—see Figs. 2 and 3).

Given this 'chemical algorithm' (Fig. 4) for constructing a model of Titan's interior, we vary the initial total mass and the rock fraction of proto-Titan, with the requirement that the final radius and density match the observed values, and that the fraction of ammonia remaining following completion of reaction (1) is precisely zero. The latter constraint is a very unlikely contingency, but it allows for future consideration of having an ammonia excess or deficit.

In constructing a structural model of Titan, the density of the core is calculated from the measured equation of state of antigorite (Hilairet et al., 2006), supported by the volume thermal expansion coefficient, and temperature dependence of the bulk modulus, $\partial K/\partial T$, for chlorite (Pawley et al., 2002); we thus adopt a mean core density of 2750 kg m^{-3}. The density of brucite is calculated from the thermal equation of state of Fukui et al. (2003), yielding a value of 2400 kg m^{-3}. The densities of ice VI and structure I methane clathrate are calculated from the parameterized equations of state in Fortes (2004), yielding mean densities of 1400 and 940 kg m^{-3}, respectively. The compressibility of aqueous ammonium sulfate has never been measured, so we use as a proxy the compressibility of eutectic $MgSO_4$ measured by Hogenboom et al. (1995); using the ambient pressure density of 1235 kg m^{-3} for the eutectic liquid (see Fig. 4), gives a mean density of 1350 kg m^{-3} for the subsurface ocean.

2.2. Model results

The observed radius and density of Titan (2575 km, 1881 kg m^{-3}) are reproduced for a fully differentiated structural model (Fig. 5) with a starting mass of 1.3567×10^{23} kg (1.0087 times larger than the final mass), and a 'rock' mass fraction of 52.8%; reaction (1) consumes all of the available ammonia when the initial NH_3 mass fraction in the volatile component is 3.1%. Insoluble hydroxides produced in reaction (1) are shown here as an accumulation on top of the hydrous silicate core; although described as a 'mud' (it would indeed have been a muddy sediment initially), the final state of the compressed and dewatered layer will be a lithified stratum. The available methane in solution in the primordial ocean can form a solid clathrate shell over 100 km thick (the final thickness, when ocean components—ice and ammonium sulfate—are intruded, is 125 km). Clathrates in terrestrial oceanic sediments form at rates from less than 100 moles m^{-2} yr^{-1} (Torres et al., 2004) up to 10,000 moles m^{-2} yr^{-1} (Haeckel et al., 2004); at the lower limit, the crust of Titan would form in ∼5 million years. The methane which is not dissolved in the ocean constitutes a massive early atmosphere; the case of NH_3:$CH_4 = 1$ that we have initially considered results in outgassing of a huge quantity of methane (19,000 km amagat, or ∼175 bar) more than 100 times greater than the current mass of Titan's entire atmosphere, and more than 6000 times the present atmospheric CH_4 inventory (roughly 3 km amagat). Relaxing the initial condition that NH_3:$CH_4 = 1$, can reduce the size of this early atmosphere (i.e., for NH_3:$CH_4 = 0.5$, the column density falls to ∼3000 km amagat, or ∼30 bar), although decreasing the ratio below 0.4 does not saturate the ocean. A large and hot primordial atmosphere will experience major—even total—loss via hydrodynamic escape, magnetospheric scavenging, and impact

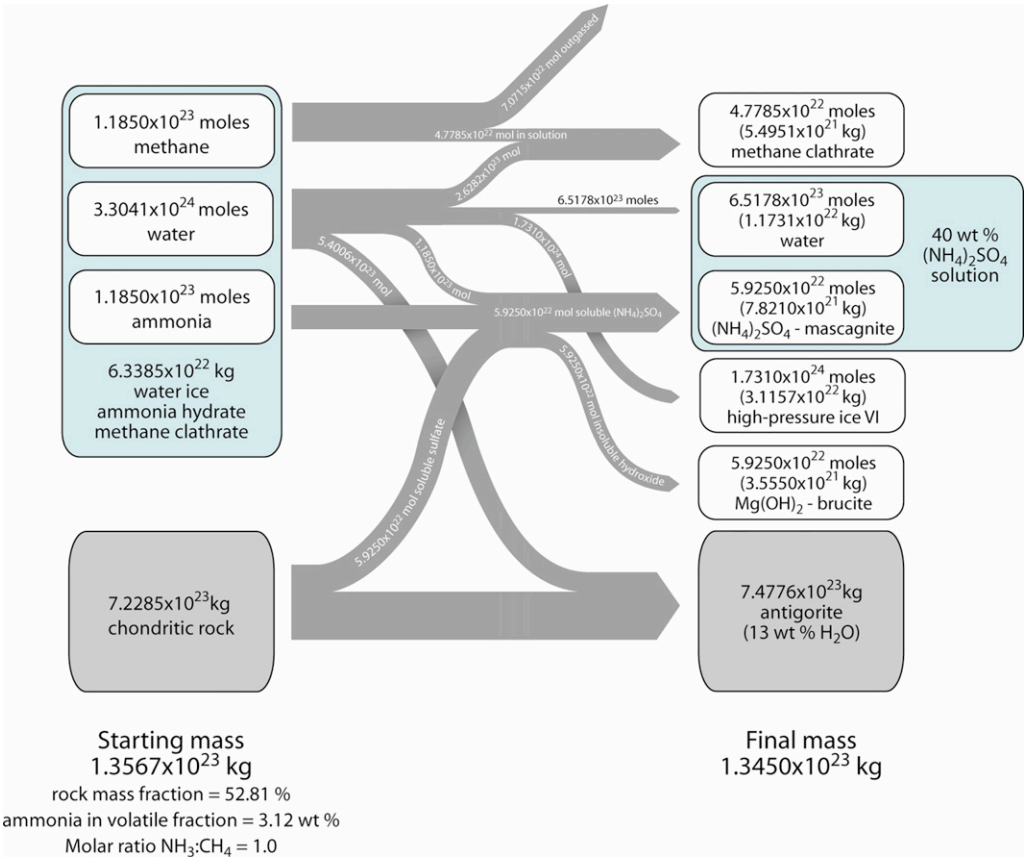

Fig. 4. The mass balance describing the chemical evolution of proto-Titan during the differentiation process, including hydration of the core, leaching of soluble sulfates, and the reaction of sulfate brines with primordial ammonia to form ammonium sulfate.

erosion (e.g., Zahnle et al., 1992). The current atmosphere may be exogenic (sourced from cometary volatiles), or endogenic (post heavy bombardment outgassing).

2.3. *The near-surface thermal structure*

For our initial rock volume of 2.41×10^{19} m^3, and a radiogenic heat production from ^{238}U, ^{232}Th, and ^{40}K equivalent to 0.010–0.015 μW m^{-3}, then the bulk global heat production, ignoring heat from tidal dissipation (see, e.g., Sohl et al., 1995, 2003), is 2.4–3.6 $\times$ 10^{11} W (or 2.9–4.3 mW m^{-2}). For a pure methane clathrate crust, with a thermal conductivity at 95 K of 0.45 W K^{-1} m^{-1} (Krivchikov et al., 2005), then the near-surface thermal gradient may be ∼6.5–9.5 K km^{-1} (compare 0.4–0.6 K km^{-1} for a bulk ice Ih shell with a thermal conductivity of 7 W K^{-1} m^{-1} at 95 K). With the impure shell proposed in Section 2.1, a thermal gradient of 4–5 K km^{-1} may be appropriate, in which case the ambient-pressure eutectic melting temperature can be reached at a depth of 30–40 km. Since the eutectic temperature in the $(NH_4)_2SO_4$–H_2O system is likely to drop by 10–20 K up to 3 kbar (reflecting the drop in T_m of ice Ih) before rising again at higher pressure, it is probable that (i) partial melting *will* occur in the outer shell, and (ii) a global subsurface ocean of eutectic liquid *might* be possible beneath the outer shell. The problem of bringing any such melts to the surface is addressed in Section 3.1. Of course, the existence and long-term stability of a global subsurface ocean is a non-trivial problem which we do not address here; these are simple first-order arguments regarding the possible occurrence of near-surface partial melting. Whilst it has been pointed out to us that 250 K is rather warm for Titan's upper mantle, such temperatures must prevail in the upper mantles of Ganymede and Callisto in order to preserve their subsurface (brine?) oceans in the probable absence of ammonia (Zimmer et al., 2000; Kivelson et al., 2002). A less conductive clathrate shell would provide greater thermal insulation for Titan's interior than an ice shell.

The structural model of Tobie et al. (2006), which is characterized by a pure CH_4-clathrate shell becomes thermally destabilized because the much greater strength of the clathrate (Durham et al., 2003) inhibits solid-state convection. The admixture of ice and ammonium sulfate in our model prevents this 'over-heating' since the minor components will melt, and thus lubricate convective motion, at temperatures much lower than the decomposition temperature of CH_4-clathrate. Tobie et al. (2006) thus predict that methane outgassing has occurred at specific periods in Titan's history: as discussed further in Section 3.2, we propose that CH_4 outgassing has been continuous, occurring when CH_4 clathrate is both warmed and decompressed (in rising cryomagma). Recent work on the mechanical properties of other solid sulfate–ice systems (McCarthy et al., submitted for publication) indicates that the bulk rheology is not simply that of the weakest component; fine-grained eutectic intergrowths result in a much stronger (and dissipative) com-

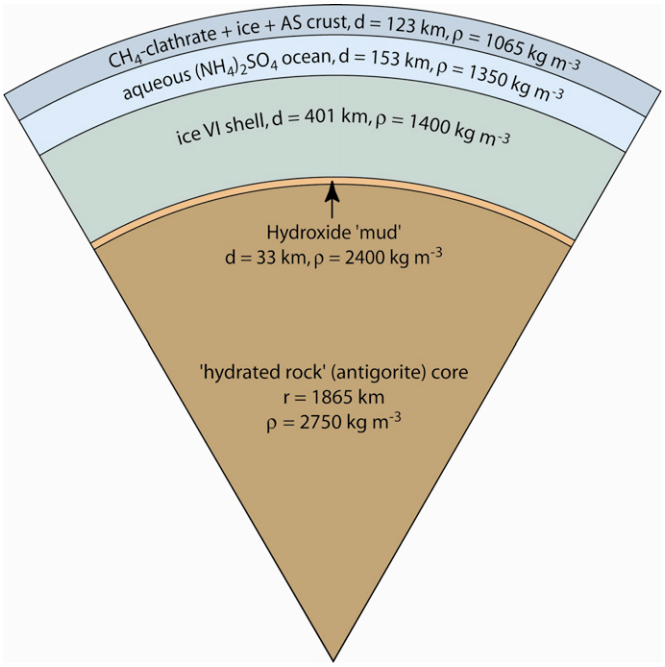

Fig. 5. The structure of Titan's interior which is consistent with the observed mass and density of the moon and with the chemical mass balance illustrated in Fig. 4. The calculated normalized moment of inertia (I/MR^2) for this model is 0.3384, and the pressures at the base of the ice VI shell, and in the center of the core, are 1.25 and 5.00 GPa, respectively. Note that this is one of a spectrum of possible models, depending on how far to the right reaction (1) proceeds, the relative abundances of reactants, and the ensuing thermal history.

posite. Thus our model shell would be stronger than pure ice (though arguably not as strong as pure clathrate), and dissipate tidal energy more readily.

3. Surface manifestation of the new internal structure

3.1. Cryovolcanism (effusive)

If ∼10% of the global heat flow of 2.4–3.6 × 10^{11} W (Section 2.3) is transported to the surface via the melting and emplacement of cryomagma, then the mass of magma produced globally is from 3.8–5.7 × 10^{12} kg year^{-1}, taking the heat of fusion ≈200 J g^{-1} for a eutectic mixture of ice and ammonium sulfate (heat of solution of $(NH_4)_2SO_4$ = 49.95 J g^{-1}; Lide, 2005), and roughly two-thirds of that for melting pure water ice (heat of fusion = 334 J g^{-1}; Lide, 2005). Even considering the lower limits of heat flow (and bearing in mind that most of the magmatism will likely be intrusive), it is apparent that Titan's radiogenic heat is sufficient to account for the existence of extensive cryolava flows. If roughly one-fifth of the total magma generated annually makes it to the surface, this could produce a single flow 75 km in length, 1 km wide, and 10 m deep (or many smaller flows) every year. The problem in terms of explaining the existence of large cryovolcanic units on Titan's surface is thus not one of energy supply, but rather one of buoyancy.

3.1.1. Eruption mechanism

Magmas produced in silicate systems typically have large negative density contrasts with the host rock ($\Delta\rho \approx$ 500–1000 kg m^{-3}), resulting in large positive (upward) buoyancy forces, and also experience greater degrees of partial melting when decompressed. In all plausible cryomagmatic systems this situation is reversed. Not only are density contrasts between partial melts and their host 'rocks' quite small (order 10s kg m^{-3}), they are often positive, meaning that partial melts will prefer to propagate *downwards* into the mantle rather than rise to the surface. Moreover, aqueous systems are faced with an effective 'wall' in the form of the negative pressure melting curve of low-pressure ice Ih; the consequence of this, should a cryomagma be able to rise towards the surface, is that it will progressively freeze as it is decompressed. In spite of this, there are abundant examples of cryomagmatism on a number of Solar System bodies, so mechanisms must exist which can overcome the impediments just described. In the case of Titan, it has been suggested that tidal pumping could bring ammonia–water liquids to the surface (Mitri et al., 2006), and for Ganymede, the formation of crustal rifts is suggested as a means of supplying hydraulic pressure gradients to force shallow (5–10 km) melts to the surface that would otherwise percolate downwards (Showman et al., 2004). In the latter case, cryomagmas are unable to overtop the graben systems because the pressure gradients are eliminated as the rifts are filled. This is a rather unusual situation (except perhaps for the uranian moon Ariel); cryomagmatic features on Triton, for example, and the few clear examples on Titan, appear not to be controlled by surface topography in the same way. The proposed cryovolcano Ganesa Macula (Lopes et al., 2007), judging by regional flow directions, appears to be situated on the flank of an uplifted area. Still, it is straightforward to determine the maximum depth from which fluids could be erupted as a result of surface topography. Showman et al. (2004) derive the following relationship:

$$d_{\max} = \frac{1}{m} \ln\left(\frac{\Delta\rho}{\rho |h_0| m}\right), \tag{1}$$

where $\Delta\rho$ is the density contrast between the melt and the matrix, ρ is the bulk density of the matrix, h_0 is amplitude of the topography, and $m = 2\pi/L$, where L is the wavelength of the topography. For our worst case, in which we wish to erupt eutectic ammonium sulfate solutions, with a density of 1235 kg m^{-3} (Fig. 2), through a crust with a bulk density of 1065 kg m^{-3}, then we obtain the result that magma may be pumped up from depths of just over 4.5 km when the topographic amplitude is 4 km ($h_0 = 2$ km) and the wavelength is 30 km (Fig. 6, line b), values which are reasonable for some of the smaller impact structures expected on Titan by virtue of atmospheric shielding. Observations to date show little evidence of short wavelength topography with amplitudes exceeding 1 km; for the case of $h_0 = 1$ km, then $d_{\max} = 2.3$ km for $L = 15$ km (Fig. 6, line a). Thus, narrow graben systems could provide the last bit of lift to liquids which have stalled near the surface, but we will show later that an alternative mechanism may dominate at depths shallower than 2 km. The circumstance investigated by Showman et al. (2004) for Ganymede, where surface topography generates the stress field to counteract the negative buoyancy of cryomagma, can be extended to include other sources of stress. These might include differential ther-

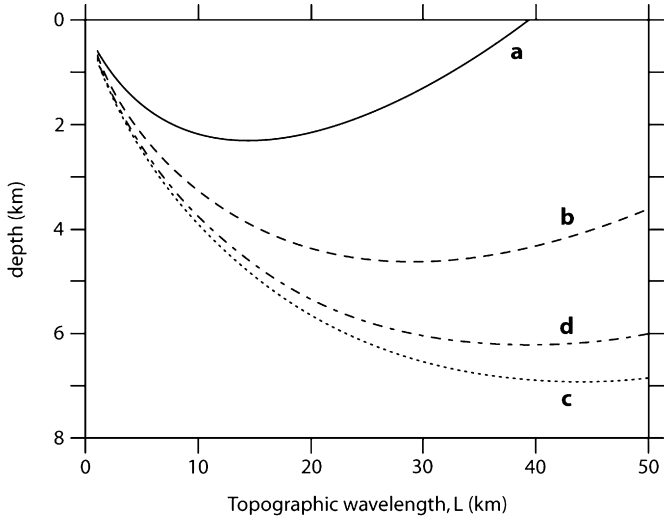

Fig. 6. The calculated depths from which cryomagmas might be pumped by stress fields due to surface topography and a rising ice diapir as a function of the wavelength and amplitude of the density disturbance. Lines a, b, and c refer to pumping by surface topography with, respectively, amplitudes of 2, 4, and 6 km (i.e., $h_0 = 1$, 2, and 3 km). $\Delta\rho = 170\ \mathrm{kg\,m^{-3}}$ for the case of eutectic ammonium sulfate, and $\rho = 1065\ \mathrm{kg\,m^{-3}}$. Line d shows the results for pumping by a rising diapir, with an amplitude of 50 km ($h_0 = 25$ km) and a density contrast between diapir and crust of $115\ \mathrm{kg\,m^{-3}}$.

mal expansion of a heterogeneous crust (the volume thermal expansion of CH_4 clathrate is roughly double that of ice Ih), and thermal or compositional convection in the supra-oceanic shell. The latter is particularly interesting because secular cooling of a subsurface ocean results in underplating of the outer shell with low-density ice Ih (the pressure is <2 kbar); the density contrast due to such underplating is much larger than that which is likely due to a thermal instability. Underplating of the supra-oceanic shell by low density ice Ih generates a gravitationally unstable state in which the accumulated ice will rise upwards through the denser overlying material. Diapiric bodies of ice will ascend, generating a stress field in the surrounding viscous material as they rise, and producing uplift (combined with radial fracturing) of the overlying brittle part of the crust. Not only will melt pockets be advected towards the surface by the rising diapir, but the buoyancy forces themselves supply a stress field that can mimic the effect of topographic pumping. The solution derived by Showman et al. (2004) can be applied to diapirism very easily by substituting for the density term in (1) with another $\Delta\rho$ to represent the density contrast between the diapir and the material through which it is rising. Because $\Delta\rho_{\mathrm{solid}}$ is a much smaller quantity ($115\ \mathrm{kg\,m^{-3}}$) than the bulk density of the matrix, this mechanism is much less efficient. However, this is compensated for to a certain extent by the greater vertical amplitude of the density disturbance compared with the surface topography: for $h_0 = 25$ km, then $d_{\max} \approx 6$ km when $L = 40$ km (Fig. 6, line d).

Compositional diapirism has been proposed as the origin of Triton's cantaloupe terrain (Schenk and Jackson, 1993), and we suggest that a similar underplating mechanism could have led to the formation of a density inversion in a supra-oceanic shell, rather than Schenk and Jackson's model in which solid CO_2 is condensed onto an ice crust. An alternate model of ice diapirism is addressed by Waltham (submitted paper) as an explanation for certain sub-circular features observed on Titan's surface.

3.1.2. Estimated effusion rates

It is also of interest to estimate the likely effusion rates necessary to produce large flow fields on the surface of Titan. The eruption of a very water-rich cryolava should rapidly lead to the development of a skin of crystalline water ice on contact with the air (N_2 at 95 K) which will not only insulate the underlying flow, but also release a considerable amount of latent heat into the flow—keeping it liquid for longer. Here, we explore a simple cooling model, which has been applied successfully to modeling terrestrial flows, for a flow 50 km long, 10 km wide, and 1 m thick, composed of (i) pure water, (ii) a eutectic 40 wt% $(NH_4)_2SO_4$ solution, and (iii) a 32.1 wt% NH_3 solution (corresponding to pure ammonia dihydrate). Assuming that the cooling is largely radiative, the effusion rate is related to the final area of the flow by an equation which balances the total emitted heat with the energy loss needed to cool the entire flow to its solidus (after Pieri and Baloga, 1984), and the latent heat of crystallization;

$$Q = \left[\frac{T_{\mathrm{solidus}}^4 \varepsilon\sigma A}{\rho(\Delta T C_P + L)}\right], \tag{2}$$

where Q is the effusion rate ($\mathrm{m^3\,s^{-1}}$) assuming that the flow's crust is thermally inhomogeneous (i.e., not broken up and continuously renewed), ε is the emissivity (assumed = 1), σ is the Stefan–Boltzmann constant ($5.67 \times 10^{-8}\ \mathrm{J\,s^{-1}\,m^{-2}\,K^{-4}}$), ρ is the density ($\mathrm{kg\,m^{-3}}$), C_P is the heat capacity ($\mathrm{J\ kg^{-1}\,K^{-1}}$), L is an effective latent heat of crystallization ($\mathrm{J\,kg^{-1}}$) of the magma, and A is the total area of the flow ($\mathrm{m^2}$). ΔT is the difference between the liquidus and the solidus, which, for pure substances or eutectic mixtures, is zero; since the melting of ammonia dihydrate is incongruent, there is a finite ΔT of ~3 K for the pure substance.

Given the exceptionally large latent heat of crystallization of ice, it is important to account for its buffering effect on the cooling of the flow; indeed for pure ice erupted at its liquidus, the only thing preventing instantaneous solidification is latent heating. Although we do not know how ammonium sulfate solutions will behave when quenched, we know from our own laboratory experience that supersaturated magnesium sulfate solutions crystallize rather than forming glasses when quenched from room temperature in liquid nitrogen (i.e., at very high rates of $>50\ \mathrm{K\,s^{-1}}$): we have observed that aqueous ammonia solutions form glasses even when cooled at rates of $0.01\ \mathrm{K\,s^{-1}}$. Our own laboratory experience with aqueous solutions of sulfuric acid and methanol are very similar, these forming a toffee-like fluid when rapidly cooled to L-N_2 temperatures. With this in mind, even if the ammonia solution partially crystallizes during ascent to the surface—as seems likely for all cryomagmas (Mitchell et al., 2006)—we would expect it to form a glassy skin when rapidly quenched in the cold air at Titan's surface, which will merely insulate the flow but not contribute any latent heat; subsequent crystallization of the flow interior (and devitrification of the crust) will probably occur so slowly that

Table 1
Calculated effusion rates necessary to produce a flow with a plan area of 50 × 10 km for various compositional parameters

Composition	$T_{solidus}$	Density ($kg\,m^{-3}$)	Heat capacity ($J\,kg^{-1}\,K^{-1}$)	Effective latent heat ($J\,kg^{-1}$)	Effusion rate ($m^3\,s^{-1}$) (50 × 10 km area)	Emplacement time (1 m thick flow)
Pure water	273.15 K	1000	4000	334×10^3	467	12.4 days
40 wt% $(NH_4)_2SO_4$	253.8 K	1235	2970	200×10^3	469	12.3 days
32.1 wt% NH_3	176.1 K	940	3150	0	3072	45.2 h

the latent heat evolved can be lost without remelting the flow. Hence we assume that ammonia hydrates crystallize so slowly that the latent heat is produced too late to contribute to the life of the flow (i.e., $L = 0$).

Input parameters and results for each case are given in Table 1. Of these three cases, the last seems very improbable. Under the low gravity at Titan's surface (1.354 $m\,s^{-2}$), a eutectic NH_3 solution will have an effective viscosity similar to that of a rhyolite on Earth (Kargel et al., 1991). Thus the emplacement of a 50 km × 10 km unit in less than two days is most unlikely. The first two cases yield more reasonable effusion rates, given an effective viscosity similar to basalt for water-rich fluids in Titan's gravity (Kargel et al., 1991). Sulfate solutions have a much lower viscosity compared to aqueous ammonia or aqueous mixtures of ammonia and methanol (Kargel et al., 1991): the eutectic viscosities of aqueous ammonium sulfate, aqueous ammonia, and aqueous ammonia–methanol are, respectively, 6 mPa s (Fig. 3), 4 Pa s, and ∼4000 Pa s (compare with 1.793 mPa s for pure water at 273.15 K). The combination of low eruption viscosity, high eruption temperature, and an ability to crystallize even when quenched very rapidly (thus providing latent heat of crystallization to the flow) means that ammonium sulfate cryomagmas *might* be a more attractive proposition than aqueous ammonia (with or without methanol) for explaining very long (ca. 100 km) flows seen east of Ganesa Macula. Of course, consideration of pure substances or mixtures at, or very close to, a eutectic (or peritectic) point results in small or vanishing values of ΔT. For the plausible case of, for example, dilute solutions of ammonia, then ΔT may be large—perhaps many tens of Kelvin—which will greatly reduce the effusion rates necessary to emplace massive flows. We have considered eutectic solutions in more detail as they are likely to be representative of small partial-melt fraction magmas: on Earth, partial-melt fractions are often very small indeed (of the order of 1%).

3.2. Cryovolcanism (explosive)

Explosive activity becomes possible if the magma contains a volatile species that is capable of exsolving as it rises towards the surface and decompresses. For Titan, plausible volatile species in the melt include methane, carbon monoxide and nitrogen. Although we will only consider the role of methane in detail, this should be viewed as the most conservative case since both N_2- and CO-clathrates decompose at much higher pressures than CH_4-clathrate at a given temperature (see below). Explosive activity may also occur when magma comes into contact with an external volatile source. In the case of a dike being forcibly intruded through a methane clathrate crust, fragments of wall rock (xenoliths) may become entrained in the magma flow. Large xenoliths may also become incorporated by stoping of magma chamber roofs. This process is practically ubiquitous in terrestrial magmatic systems (e.g., Dawson, 1980; Nixon, 1987) and may well play a role in cryovolcanism on Enceladus: the measured abundances of CH_4 and N_2 relative to water in the Enceladus south polar plume (1.6 and 4%, respectively; Waite et al., 2006) are roughly an order of magnitude larger than the plausible solubility of these species in water (O'Sullivan and Smith, 1970); the only means of incorporating these quantities into the erupted material is from clathrate xenoliths (cf., Prieto-Ballesteros and Kargel, 2006).

Finally, explosive activity may occur where a magmatic dike is intruded into volatile-laden sediments (such as those observed at the Huygens landing site; Niemann et al., 2005), or where liquid methane seeps down into fractured bedrock, coming into contact with plutonic bodies. Seepage of liquid methane into fractured bedrock which is 'geothermally' heated by an underlying pluton could result in geysering, as considered previously by Lorenz (2002).

We model the two principal methods of introducing methane into the rising cryomagma: (i) in solution; and (ii) in the form of methane clathrate xenoliths. These form the basis for a range of model scenarios. We consider two magma compositions, the first with a density equal to the bulk density of the model crust (1065 $kg\,m^{-3}$), and the second being a eutectic liquid in the binary $(NH_4)_2SO_4$–H_2O system ($\rho = 1235\ kg\,m^{-3}$). The less dense liquid corresponds to a composition of 10.6 wt% $(NH_4)_2SO_4$, the liquidus temperature being 270.7 K, and the viscosity 2.16 mPa s (crystal free liquid). The denser liquid has a composition of 40 wt% $(NH_4)_2SO_4$, and is erupted at a temperature of 253.8 K with a viscosity of 6.12 mPa s (crystal free liquid). The solubility of methane in these two liquids as a function of pressure is estimated from the solubility of methane in, respectively, 1 and 4 M NaCl solutions (Duan et al., 1992), which have water activities comparable to the two magma compositions; in the case of the 4 M solution, we have extrapolated the solubility to 253 K. The clathrate decomposition pressure is also affected by the presence of dissolved salts, and we have assumed that the dissociation temperature depression is 0.65 times the freezing point depression in the gas-free system (cf., Nielsen and Bucklin, 1983; Sloan, 1990): the estimated clathrate dissociation pressures are therefore 2.52 MPa in the 10.6 wt% solution (equivalent to a depth of 1750 m), and 2.04 MPa in the eutectic solution (equivalent to a depth of 1415 m). The decomposition of entrained xenoliths immediately liberates methane gas into the melt over

and above that already exsolved (or not) from solution. In a eutectic magma (at 253 K) clathrate grains will dissociate in a matter of just a couple of minutes (cf., Takeya et al., 2002). Note that in ammonia–methanol–water magmas, at temperatures of ~150 K (Kargel, 1991), clathrate grains may barely dissociate at all over a period of several weeks; in the absence of methanol (i.e., at 175 K), then the time required is order 10^4 s, or ~7 days (Takeya et al., 2002). The experimental dissociation times cited by Takeya et al. (2002) pertain to particles 20–50 μm in diameter; millimeter to centimeter-sized xenoliths will require much longer to fully degass, the process being slowed by the requirement that methane diffuse through a thickening crust of ice (although the crust may dissolve in, or be mechanically abraded by the surrounding magma). With this in mind, we would go as far as to suggest that explosive volcanism in ammonia–water, or ammonia–methanol–water systems, is impossible. In other words, evidence for explosive activity could effectively rule out these compositions.

For both the 10.6 and 40.0 wt% magmas we have modeled two extreme situations, one in which the liquid is saturated with methane in the source region (arbitrarily chosen as being at 20 km depth), and one in which the liquid contains no methane. For both situations, we also consider the effect of incorporating variable mass fractions of entrained clathrate xenoliths. Clearly, for the case in which the liquid contains no dissolved methane, no explosive activity can be realized until some critical xenolith abundance is reached. Realistically, partial melts are most unlikely to be saturated with methane; assuming that liquids are able to equilibrate with methane clathrate in the source region, the likely quantity of dissolved methane will be very small (order 0.1 wt%; Handa, 1990).

As the magma rises towards the surface, the confining pressure decreases, thus reducing the solubility of methane in the liquid, resulting in exsolution and the nucleation and growth of gas bubbles. If the total gas bubble volume fraction becomes large enough (~60–85%) then the magma is said to fragment, powering a Hawaiian-style explosive eruption (Pinkerton et al., 2002; Head and Wilson, 2003; Parfitt, 2004). If the magma viscosity is higher, bubbles may coalesce, driving strombolian-type activity. In extreme cases, blocking of the vent can result in build up of gas-laden foam, or the prevention of gas exsolution. Sufficient pressure may accumulate to destroy explosively the vent blockage; sudden pressure release may result in violent degassing of the magma, as occurred at Mount St. Helens in 1980, for example.

Using the model described in Pinkerton et al. (2002) and Head and Wilson (2003), the exsolved methane mass fraction (n_m) provides the bulk magma density (β), and the bubble volume fraction (V_b);

$$\beta^{-1} = \left[(n_m RT)/mP\right] + \left[(1-n_m)/\rho\right], \tag{3}$$

$$V_b = 1 - \beta\left[(1-n_m)/\rho\right], \tag{4}$$

where P and T are pressure and temperature, respectively, R is the gas constant (8.314 J K^{-1} mol^{-1}), m is the molar mass of the volatile species (methane = 0.016 kg mol^{-1}), and ρ is the density of the bubble-free magma. Explosive disruption is considered to occur at the pressure, and hence depth, where the bubble volume fraction reaches either 60 or 75%. The former reflects the likelihood that very low viscosity melts will disrupt more easily, and the latter is for consistency with studies of terrestrial magmas. We then use the fragmentation pressure to determine the velocity of the erupted gas and cryoclastic material through the vent (Head and Wilson, 2003);

$$0.5u^2 = \frac{n_m RT}{m}\ln\left(\frac{P_F}{P_V}\right) + \Delta P\left[\left(\frac{1-n_m}{\rho_{\text{magma}}}\right) - \frac{1}{\rho_{\text{crust}}}\right], \tag{5}$$

where P_F and P_V are fragmentation and vent pressures, respectively (and $\Delta P = P_F - P_V$), and the other terms have the same meaning as in Eqs. (3) and (4). This yields an estimate of how high may be the resulting lava fountain via the ballistic equation ($H = u^2/2g$, where H = lava fountain height, u = vent eruption velocity, and g = acceleration due to gravity, 1.354 m s^{-2}).

Table 2 summarizes the results for each scenario, except scenario 4, where explosive activity for $V_b = 0.75$ can only occur at xenolith abundances greater than 0.10 wt%. Introduction of clathrate xenoliths dramatically increases the explosivity of eruptions—producing ice lava fountains a few kilometers high even for xenolith abundances of just a few wt%. For magmas containing no dissolved methane (scenarios 3 and 6), the critical xenolith contents for fragmentation are 1.12 wt% ($V_b = 0.60$) or 2.24 wt% ($V_b = 0.75$) for the 10.6 wt% liquid, and 1.03 wt% ($V_b = 0.60$) or 2.06 wt% ($V_b = 0.75$) for the eutectic liquid. Given the very low levels of clathrate entrainment necessary to produce fragmentation, it seems that vigorous explosive cryovolcanism may be the norm rather than the exception on Titan.

Table 2
Calculated cryomagma disruption properties for a range of dissolved methane/entrained clathrate scenarios

	For fragmentation at $V_b = 0.60$			For fragmentation at $V_b = 0.75$		
	Fragmentation depth (m)	Eruption velocity (m s^{-1})	Lava fountain height (m)	Fragmentation depth (m)	Eruption velocity (m s^{-1})	Lava fountain height (m)
1	272	32.8	397	138	17.8	117
2	1194	109.0	4390	604	92.6	3167
3	940	90.9	3053	470	75.3	2095
4	196	20.1	148	–	–	–
5	1218	99.6	3660	606	85.0	2666
6	1019	87.6	2833	510	73.7	2007

1: 10.6 wt% solution, saturated with CH_4, no xenolith entrainment. 2: 10.6 wt% solution, saturated with CH_4, but with 10 wt% entrained xenoliths. 3: 10.6 wt% solution, with no dissolved CH_4 and 10 wt% entrained xenoliths. 4: 40.0 wt% solution, saturated with CH_4, no xenolith entrainment. 5: 40.0 wt% solution, saturated with CH_4, but with 10 wt% entrained xenoliths. 6: 40.0 wt% solution, with no dissolved CH_4 and 10 wt% entrained xenoliths.

Recall that this is a conservative result. CO-clathrates dissociate at pressures of 8.57 MPa (Mohammadi et al., 2005), and N_2-clathrates at 12.30 MPa (Sloan, 1990), at 270 K in pure water. Therefore, these will break down at much greater depths, 6–8 km, providing a mechanism for erupting dense cryomagmas, and for generating large eruption plumes.

4. Discussion

4.1. Surface composition and geology

In the foregoing sections, we have predicted that Titan's crustal bedrock is composed of a heterogeneous mixture of methane clathrate, ice, and ammonium sulfate (or its tetrahydrate). Over time, aqueous solutions of ammonium sulfate have been explosively erupted onto the surface. We must now ask whether or not there is observational evidence to test this hypothesis.

Compositional evidence regarding the surface of Titan comes from Earth-based telescopic observations (e.g., Coustenis et al., 2006) and from a suite of instruments comprising the Cassini–Huygens spacecraft. These include the Visible and Infrared Mapping Spectrometer (VIMS; Brown et al., 2004) aboard Cassini, and the Descent Imager and Spectral Radiometer (DISR; Tomasko et al., 2002) which was carried to Titan's surface by Huygens in January 2005. Additionally, the 0.938 μm channel of the Cassini Imaging Science System (ISS; Porco et al., 2004) is able to see the surface at high spatial resolution. Less direct, compositional information is encoded in the electrical properties of the surface as probed by the Cassini radar system (Elachi et al., 2004).

The diffuse near infrared reflection spectrum of ammonium sulfate (Clark et al., 2003) is remarkably similar to that of ice in the region observed by the Huygens DISR, having absorption bands centered at similar wavelengths (Fig. 7). It is therefore a credible candidate for the unidentified IR-blue component

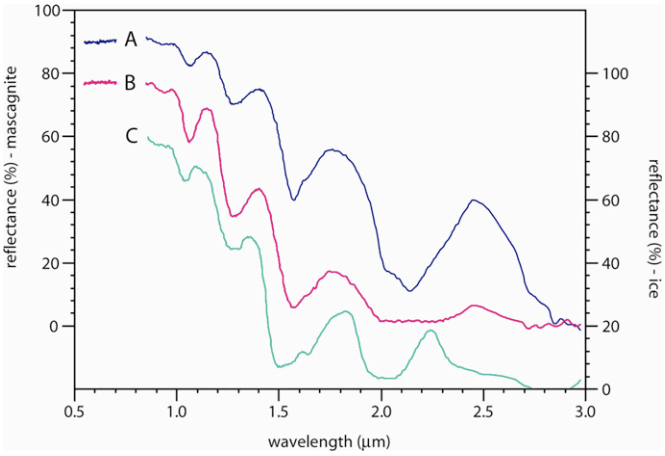

Fig. 7. The near-IR spectra of fine-grained and coarse-grained $(NH_4)_2SO_4$ (lines A and B, respectively) at 1 bar, 298 K (GDS-65.4315 and GDS-65.4303), compared with the spectrum of water ice at 77 K (line C, GDS-136.9212). Plotted from data in the USGS Digital Spectral Library (Clark et al., 2003). Ammonium sulfate reflectances are plotted on the left ordinate, and those of ice on the right.

of the surface spectrum at the Huygens landing site (Tomasko et al., 2005). Although the reflection spectrum of ammonium sulfate in the mid-infrared region sampled by VIMS appears not to have been measured, the transmission spectrum exhibits no absorption features at 5 μm (Schutte and Heyns, 1970), and the sulfates of other monovalent cations (such as Na_2SO_4 and K_2SO_4) have IR reflectances at 5 μm of ∼40%, becoming smaller as the hydration number increases (Clark et al., 2003). The IR reflectance of ice is roughly 3% at this wavelength (Salisbury et al., 1994). From this we infer that ammonium sulfate tetrahydrate will have a 5 μm reflectance of 10–15%, also making it a viable candidate for the 5 μm-bright material described by Barnes et al. (2005).

If the primitive ammonia abundance is smaller than 2 wt%, then Titan's interior may resemble the models of Ganymede described by Kargel (1991). The likely compounds that could be dissolved in cryovolcanic liquids tend to crystallize as hydrates ($MgSO_4{\cdot}nH_2O$, $Na_2SO_4{\cdot}nH_2O$, $Na_2CO_3{\cdot}nH_2O$, $H_2SO_4{\cdot}nH_2O$) with large hydration numbers, $n = 6$–11. Each of these will have mid-IR reflectivities similar to water, not to mention greatly distorted absorption bands in the region accessible to DISR.

Given the very large difference in density between ice ($\rho_{ice} = 930\ kg\,m^{-3}$ at 95 K) and ammonium sulfate ($\rho_{AS} \approx 1790\ kg\,m^{-3}$ at 95 K: Hoshino et al., 1958), both fluvial and aeolian processes will very effectively separate the two minerals. Thus, we should expect ammonium sulfate to form the major lag deposit on the higher terrain (and the first airfall from cryoclastic clouds), whereas ice should be more easily transported. Indeed the obvious IR contrast between the 'dark' and 'light' terrains in ISS images of Titan might be attributed to such differences in transport efficiency. The less dense mineral, ice, will be more readily transported and accumulated in sedimentary basins (and thus appear IR-dark) whereas a lag of IR-brighter sulfate would be left at higher elevations. The sedimentary material likely appears dark at visible wavelengths because of the accumulation of organic matter—'tholins'—that are relatively bright in the infrared. If, as we predict, volcanic activity is dominantly explosive, a large quantity of dust-sized material could be carried to high altitudes in warm eruption clouds. Long-distance transport by Hadley-style meridional circulation could result in dust being deposited poleward of a major eruption event, and indeed being preferentially deposited where the air descends at the poles. Hence the polar regions may appear brighter at 5 μm because of an accumulation of volcanic dust.

Information about the electrical properties of Titan's surface is extracted from radar scatterometry and radiometry. So far, the two methods are yielding different model dielectric constants (Elachi et al., 2005, 2006; Paganelli et al., 2006; Wye et al., 2006); generally the dielectric constants from the scatterometry are 2–6, and from radiometry the values are 1–2. These discrepancies might be accounted for by volume scattering within radar transparent near-surface materials: the backscatter power of bright areas in SAR data can be matched by water ice + ammonia hydrates with large volume scattering terms (Paillou et al., 2006). At Titan's surface temperature, the real part of the dielectric constant, ε, of ammonium sul-

fate in its ferroelectric phase is ≈5.5 (Hoshino et al., 1958), which is somewhat larger than other candidate surface materials (Thompson and Squyres, 1990), but still consistent with the observations. The presence of highly vesicular 'pumice' (which would lower the bulk density of the regolith), and also the deposition of thin 'ash' blankets (altering the effective incidence angle of the radar beam) are likely to play a role in modifying the electric response of Titan's surface.

Explosive activity would produce a range of geological landforms, some of which may be difficult to distinguish, genetically, from landforms produced by effusive activity. Normally we would expect to observe explosion craters (calderas), ash cones and ash flows. Fields of airfall ash surrounding a cone might be very flat and smooth, appearing dark in Cassini SAR images. Major explosive eruptions could result in the 'cold' equivalent of a nuée ardente with dense cryoclastic material flowing down the flanks of the volcano (carving channel-like features) and running out, perhaps for many tens of kilometers. Icy ignimbritic deposits would mantle (and soften) the landscape: Croft (1990) identified cryoclastic deposits on Triton on the basis of softened terrain and feathered edges to flow units. This may not be diagnostic in the case of flows on Titan, due to the likely transparency of ice at the radar wavelength.

At present, the most convincing candidate for a cryovolcano is Ganesa Macula, a 180-km diameter feature observed in the Ta SAR swath (Elachi et al., 2005; Lopes et al., 2007) This feature has been interpreted by different workers to be dome-like or shield-like; nonetheless it is the apparent source of a series of flow units extending over 100 km to the east. The edifice appears to us to be topped by a caldera-like feature 20 km × 10 km, within which sits a steep cone. The caldera rim is the source of several channels which are mostly (but not exclusively) observed on the eastern and south-eastern flanks. One such channel on the south-eastern flank seems to have drained south-east to form a radar-bright flow unit. In overall size and appearance, we believe that Ganesa quite closely resembles the martian volcano Ceraunius Tholus, the closest cryovolcanic analogues possibly being the large tritonian paterae, Kibu and Leviathan. It is possible that the purported flank channels are the result of dense cryoclastic flows from collapsing explosion columns; these flows have subsequently run-out to the east of the edifice, contributing to a complex pattern of radar-bright flow-like units. The asymmetry in the distribution of the channels may simply reflect a tendency of the eruption columns to collapse in a down-wind direction (assuming generally prograde near-surface winds). The summit caldera and steep cone may then be evidence of explosive collapse and resurgence. Two other crater-form features with associated flows in the Ta SAR swath may be explosion craters or examples of volcanic edifices that have experienced flank collapse as trapped magma has devolatilized. Small crater-like features in the T7 and T8 SAR swaths (Wood et al., 2006) are possible examples of explosion craters; the so-called 'ink spots' may be ash cones. It is also interesting to note that these features occur in association with arcuate mountain belts (Wood et al., 2006; Radebaugh et al., 2006). One explanation for these mountain belts is that they are the result of crustal deformation by ice diapirs, their dimensions (50–150 km) being comparable to the likely deformation wavelength for convective motions in a 100 km-thick shell. From this perspective, the ridges in Triton's cantaloupe terrain may be the closest genetic analogues to Titan's ridges (cf., Schenk and Jackson, 1993).

Cryoclastic volcanism could supply large quantities of finely comminuted vesicular 'ash' to the surface sediment reservoir. Much of this material may become cemented by the overgrowth of N_2-clathrate while it is still relatively warm, a process which can take up a significant amount of atmospheric gases (Fortes and Stofan, 2005; Osegovic and Max, 2005). Lightly welded cryotephra will probably be more erodible than polycrystalline ice. Uncemented cryotephra may be mobilized easily by liquid methane as 'mud' flows, or cryolahars. The conclusion must be that cryoclastic volcanism results in Titan's surface bearing more sedimentary material than it might do otherwise, a factor perhaps in forming the widespread dune fields observed in SAR imagery (Lorenz et al., 2006). Fluvial erosion is clearly an effective process on Titan (Lorenz and Lunine, 1996) provided there is a source of bedload material (Collins, 2005). The presence of dunes (which requires sand-sized grains) is difficult to understand if the only source of sediment is micron-sized organic aerosol particles produced by CH_4 photolysis in the stratosphere. Earlier, we derived a rough estimate of the rate at which material may be erupted onto Titan's surface (order 10^8–10^9 $m^3\,yr^{-1}$). If we were to assume that just 1000th of this material were emplaced explosively as fine grained ash, then the 10^4–10^5 km^3 of sedimentary material contained in Titan's dunes (Lorenz et al., 2006) could be accumulated in $\sim 10^4$–10^6 yr.

4.2. Atmosphere

Cryovolcanism is one mechanism for replacing methane which is irreversibly lost from the stratosphere as a result of photochemical reactions. If we assume that cryovolcanism is the sole resupply mechanism, then for reasonable global magma extrusion rates of up to $\sim 1.0 \times 10^{12}$ $kg\,yr^{-1}$, the photolytic destruction of atmospheric methane (see Lara et al., 1996) may *just* be buffered if the magma is saturated with methane in the source region (i.e., the magma contains 0.5 wt% CH_4).[1] If the magma contains a more realistic 0.1 wt% CH_4, then it is necessary to entrain and decompose 3–4 wt% of methane clathrate xenoliths: such values of xenolith abundance (which are perfectly reasonable xenolith abundances in terrestrial magmas) will lead to vigorously explosive volcanic eruptions. It is plausible that a sizable quantity of liquid methane exists in Titan's crust, either in sedimentary basins, or in deeper crustal reservoirs (e.g., Kossacki and Lorenz, 1996), which is able to resupply the atmosphere. It is possible that this reservoir is maintained in a steady state (over the long term) by volcanic resupply. However, the near-surface methane inventory may experience large short-term variability which is a function of

[1] The net CH_4 destruction rate of 7.97×10^9 molecules $cm^{-2}\,s^{-1}$ (Lara et al., 1996) corresponds to 5.564×10^9 $kg\,yr^{-1}$, which can consume 3 km amagat of methane in 32 million years.

volcanic periodicity. Episodes of vigorous volcanic outgassing, characterized by intense fluvial activity (Lorenz et al., 2005) and replenishment of aquifers, could by interspersed with periods of very low activity, characterized by 'drought' conditions, dry channels, and a rapid loss of surface liquids (e.g., Mitri et al., 2007). It may be no coincidence that the 5 μm-bright regions, Hotei Arcus and Tui Regio, are at roughly the same latitude as observed methane cloud outbursts (Griffith et al., 2005; Roe et al., 2005; Schaller et al., 2006).

5. Summary

A volatile-rich (CH_4, NH_3) proto-Titan, assuming relatively low temperature hydrothermal alteration of the silicate component, may have a subsurface ocean of aqueous ammonium sulfate beneath a thick shell of methane clathrate and ice. Measurements of the tidal variation in the 2nd order gravitational moments (Rappaport et al., 1997; Castillo et al., 2002) may show that the ocean is present: the first of three dedicated gravity flybys took place recently (T12, April 30th, 2006). The large electrical conductivity of aqueous ammonium sulfate ($\sim$300 mS cm^{-1} at the eutectic, compared with 50 mS cm^{-1} for seawater) may mean that magnetometry can detect weak induced currents from the ocean, even though the driving field, $\Delta\mathbf{B}$, is much smaller than for the Galilean moons. Improved measurements of the solid-state rheology of methane clathrate, and of clathrate-ice intergrowths, are essential for modeling the tidal dissipation which may be required to explain the persistence of a very warm (i.e., ammonia free) subsurface ocean.

Thermal and compositional convection in Titan's outer shell may advect liquid pockets close enough to the surface for stress fields (due to topography and the rise of the diapir itself) to pump the dense liquids to the surface. In the process, fragments of methane clathrate can become entrained in the melt and be transported upwards. At pressures below $\sim$2 MPa, the clathrate xenoliths decompose, releasing gas into the magma which powers explosive eruptions at the surface, with lava fountains perhaps several thousand meters high. We predict that Titan has been extensively resurfaced by lavas composed of aqueous ammonium sulfate, and by huge quantities of easily eroded cryotephra consisting of ice and ammonium sulfate (or its tetrahydrate), potentially providing a source of sediment for the observed dune fields. Both fluvial and aeolian processes will very effectively separate the two minerals. Thus, we should expect ammonium sulfate to form the major lag deposit on the higher terrain (and the first airfall from cryoclastic clouds), whereas ice should be more easily transported, and this could account for the contrast (in the infrared) between the dark and light terrains seen in ISS images. Ammonium sulfate may also be a candidate for the 5 μm-bright material on Titan, and the unidentified IR-blue component at the Huygens landing site. Unambiguously cryoclastic features might yet be observed in Cassini SAR imagery, although there are many tantalizing small crater-like features in swaths collected so far. However, a future mission to Titan will be needed to characterize these features in adequate detail, investigating the small-scale morphology of flow units (particularly possible small ash cones and spatter deposits), as well as the mineralogy, grain size and vesicle size of cryovolcanic deposits. The latter will require the capacity to image samples on microscopic scales, and possibly the ability to make in situ X-ray diffraction measurements. Further laboratory work to understand the binary system $(NH_4)_2SO_4$–H_2O at high pressure (solubility, density and viscosity) are needed, and the reported tetrahydrate phase needs characterizing (crystal structure and phase relations at low and high pressure). The mid-infrared reflection spectra of both phases need to be measured in order to draw comparisons with the observed 5 μm brightness of Titan's surface. Lastly, a subsurface ocean of aqueous ammonium sulfate (saturated with methane) provides a possible habitat for life not too dissimilar from terrestrial cold seeps (cf., Knittel et al., 2005; see also Fortes, 2000).

Acknowledgments

A.D.F. and P.M.G. are funded by the Particle Physics and Astronomy Research Council (PPARC, UK), PPA/P/S/2003/00247 and PP/C501992/1, respectively, and S.K.T. is funded by a postgraduate studentship from the Engineering and Physical Sciences Research Council (EPSRC, UK). The authors wish to thank Frederik Simons for a useful discussion about the pumping of cryomagmatic fluids by diapiric stresses, Slava Solomatov and one anonymous referee for incisive comments on the manuscript. We also thank everyone involved with the Cassini–Huygens mission to Saturn.

References

Anders, E., Grevesse, N., 1989. Abundances of the elements: Meteoritic and solar. Geochim. Cosmochim. Acta 53 (1), 197–214, doi:10.1016/0016-7037(89)90286-X.

Angel, R.J., Frost, D.J., Ross, N.L., Hemley, R., 2001. Stabilities and equations of state of dense hydrous magnesium silicates. Phys. Earth Planet. Int. 127, 181–196, doi:10.1016/S0031-9201(01)00227-8.

Atreya, S.K., Donahue, T.M., Kuhn, W.R., 1978. Evolution of a nitrogen atmosphere on Titan. Science 201 (4356), 611–613.

Bai, T.B., Koster van Groos, A.F., 1998. Phase relations in the system MgO–NaCl–H_2O: The dehydroxylation of brucite in the presence of NaCl–H_2O fluids. Am. Mineral. 83, 205–212.

Barnes, J.W., and 34 colleagues, 2005. A 5-micron bright spot on Titan: Evidence for surface diversity. Science 310, 92–95, doi:10.1126/science.1117075.

Bird, M.K., Huchtmeier, W.K., Gensheimer, P., Wilson, T.L., Janardhan, P., Lemme, C., 1997. Radio detection of ammonia in Comet Hale–Bopp. Astron. Astrophys. 325 (1), L5–L8.

Brown, R.H., Baines, K.H., Bellucci, G., Bibring, J.-P., Buratti, B.J., Capaccioni, F., Cerroni, P., Clark, R.N., Coradini, A., Cruikshank, D.P., Drossart, P., Formisano, V., Jaumann, R., Langevin, Y., Matson, D.L., McCord, T.B., Mennella, V., Miller, E., Nelson, R.M., Nicholson, P.D., Sicardy, B., Sotin, C., 2004. The Cassini Visual and Infrared Mapping Spectrometer (VIMS) investigation. Space Sci. Rev. 115, 111–168, doi:10.1007/s11214-004-1453-x.

Castillo, J., Rappaport, N., Mocquet, A., Sotin, C., 2002. Clues on Titan's internal structure from Cassini–Huygens mission. Lunar Planet. Sci. XXXIII. Abstract 1989.

Castillo, J.C., Matson, D.L., Sotin, C., Johnson, T.V., Lunine, J.I., Thomas, C., 2006. A new understanding of the internal evolution of Saturn's icy satellites from Cassini observations. Lunar Planet. Sci. XXXII. Abstract 2200.

Clark, R.N., Swayze, G.A., Wise, R., Livo, K.E., Hoefen, T.M., Kokaly, R.F., Sutley, S.J., 2003. USGS Digital Spectral Library, USGS Open File Report 03-395. http://pubs.usgs.gov/of/2003/ofr-03-395/.

Collins, G.C., 2005. Relative rates of fluvial bedrock incision on Titan and Earth. Geophys. Res. Lett. 32, doi:10.1029/2005GL024551. Article L22202.

Coustenis, A., Negrão, A., Salama, A., Schulz, B., Lellouch, E., Rannou, P., Drossart, P., Encrenaz, T., Schmitt, B., Boudon, V., Nikitin, A., 2006. Titan's 3-micron spectral region from ISO high-resolution spectroscopy. Icarus 180 (1), 176–185, doi:10.1016/j.icarus.2005.08.007.

Croft, S.K., 1990. Physical cryovolcanism on Triton. Lunar Planet. Sci. XXI, 246–247.

Dalton III, J.B., 2003. Spectral behavior of hydrated sulfate salts: Implications for Europa mission spectrometer design. Astrobiology 3, 771–784, doi:10.1089/153110703322736097.

Dalton III, J.B., Prieto-Ballesteros, O., Kargel, J.S., Jamieson, C.S., Jolivet, J., Quinn, R., 2005. Spectral comparison of heavily hydrated salts with disrupted terrains on Europa. Icarus 177 (2), 472–490, doi:10.1016/j.icarus.2005.02.023.

Dawson, J.B., 1980. Kimberlites and Their Xenoliths. Springer-Verlag, New York.

Duan, Z., Møller, N., Greenberg, J., Weare, J.H., 1992. The prediction of methane solubility in natural waters to high ionic strength from 0 to 250 °C and from 0 to 1600 bar. Geochim. Cosmochim. Acta 56 (4), 1451–1460, doi:10.1016/0016-7037(92)90215-5.

Durham, W.B., Kirby, S.H., Stern, L.A., Zhang, W., 2003. The strength and rheology of methane clathrate hydrate. J. Geophys. Res. 108 (B4), doi:10.1029/2002JB001872. Article 2182.

Elachi, C., Allison, M.D., Borgarelli, L., Encrenaz, P., Im, E., Janssen, M.A., Johnson, W.T.K., Kirk, R.L., Lorenz, R.D., Lunine, J.I., Muhleman, D.O., Ostro, S.J., Picardi, G., Posa, F., Rapley, C.G., Roth, L.E., Seu, R., Soderblom, L.A., Vetrella, S., Wall, S.D., Wood, C.A., Zebker, H.A., 2004. Radar: The Cassini Titan radar mapper. Space Sci. Rev. 115, 71–110, doi:10.1007/s11214-004-1438-9.

Elachi, C., and 34 colleagues, 2005. Cassini radar views of the surface of Titan. Science 308, 970–974, doi:10.1126/science.1109919.

Elachi, C., and 34 colleagues, 2006. Titan radar mapper observations from Cassini's T3 fly-by. Nature 441, 709–713, doi:10.1038/nature04786.

Engel, S., Lunine, J.I., Norton, D.L., 1994. Silicate interactions with ammonia–water fluids on early Titan. J. Geophys. Res. 99 (E2), 3745–3752, doi:10.1029/93JE03433.

Fortes, A.D., 2000. Exobiological implications of a possible subsurface ocean inside Titan. Icarus 146 (2), 444–452, doi:10.1006/icar.2000.6400.

Fortes, A., 2004. Computational and Experimental Studies of Solids in the Ammonia–Water System. Ph.D. thesis. University of London.

Fortes, A.D., Stofan, E.R., 2005. Clathrate formation in the near-surface environment of Titan. Lunar Planet. Sci. XXXVI. Abstract 1123.

Fukui, H., Ohtaka, O., Suzuki, T., Funakoshi, K., 2003. Thermal expansion of $Mg(OH)_2$ brucite under high pressure and pressure dependence of entropy. Phys. Chem. Miner. 30, 511–516, doi:10.1007/s00269-003-0353-z.

Grasset, O., Sotin, C., 1996. The cooling rate of a liquid shell in Titan's interior. Icarus 123 (1), 101–112, doi:10.1016/icar.1996.0144.

Grasset, O., Sotin, C., Dechamps, F., 2000. On the internal structure and dynamics of Titan. Planet. Space Sci. 48 (7-8), 617–636, doi:10.1016/S0032-0633(00)00039-8.

Greinert, J., Artemov, Y., Egorov, V., De Batist, M., McGinnis, D., 2006. 1300-m-high rising bubbles from mud volcanoes at 2080 m in the Black Sea: Hydroacoustic characteristics and temporal variability. Earth Planet. Sci. Lett. 244, 1–15, doi:10.1016/j.epsl.2006.02.011.

Griffith, C.A., and 26 colleagues, 2005. The evolution of Titan's mid-latitude clouds. Science 310, 474–477, doi:10.1126/science.1117702.

Haeckel, M., Suess, E., Wallmann, K., Rickert, D., 2004. Rising methane gas bubbles form massive hydrate layers at the seafloor. Geochim. Cosmochim. Acta 68 (21), 4335–4345, doi:10.1016/j.gca.2004.01.018.

Handa, Y.P., 1990. Effect of hydrostatic pressure and salinity on the stability of gas hydrates. J. Phys. Chem. 94 (6), 2652–2657, doi:10.1021/j100369a077.

Head, J.W., Wilson, L., 2003. Deep submarine pyroclastic eruptions: Theory and predicted landforms and deposits. J. Volcanol. Geoth. Res. 121 (3–4), 155–193, doi:10.1016/S0377-0273(02)00425-0.

Hilairet, N., Daniel, I., Reynard, B., 2006. Equation of state of antigorite, stability field of serpentines, and seismicity in subduction zones. Geophys. Res. Lett. 33, doi:10.1029/2005GL024728. Article L02302.

Hogenboom, D.L., Kargel, J.S., Ganasan, J.P., Lee, L., 1995. Magnesium sulfate–water to 400 MPa using a novel piezometer: Densities, phase equilibria, and planetological implications. Icarus 115 (2), 258–277, doi:10.1016/icar.1995.1096.

Hoshino, S., Vedam, K., Okaya, Y., Pepinsky, R., 1958. Dielectric and thermal study of $(NH_4)_2SO_4$ and $(NH_4)_2BeF_4$ transitions. Phys. Rev. 112 (2), 405–412, doi:10.1103/PhysRev.112.405.

Hunten, D.M., Tomasko, M.G., Flasar, F.M., Samuelson, R.E., Strobel, D.F., Stevenson, D.J., 1984. Titan. In: Gehrels, T., Matthews, M.S. (Eds.), Saturn. Univ. of Arizona Press, Tucson, pp. 671–759.

Iro, N., Gauthier, D., Hersant, F., Bockelée-Morvan, D., Lunine, J.I., 2003. An interpretation of the nitrogen deficiency in comets. Icarus 161 (2), 511–532, doi:10.1016/S0019-1035(02)00038-6.

Kargel, J.S., 1991. Brine volcanism and the interior structures of asteroids and icy satellites. Icarus 94 (2), 369–390, doi:10.1016/0019-1035(91)90235-L.

Kargel, J.S., 1992. Ammonia–water volcanism on icy satellites: Phase relations at 1 atmosphere. Icarus 100 (2), 556–574, doi:10.1016/0019-1035(92)90118-Q.

Kargel, J.S., Kaye, J.Z., Head, J.W., Marion, G.M., Sassen, R., Crowley, J.K., Prieto-Ballesteros, O., Grant, S.A., Hogenboom, D.L., 2000. Europa's crust and ocean: Origin, composition, and the prospects for life. Icarus 148 (1), 226–265, doi:10.1006/icar.2000.6471.

Kargel, J.S., Croft, S.K., Lunine, J.I., Lewis, J.S., 1991. Rheological properties of ammonia–water liquids and crystal–liquid slurries: Planetological applications. Icarus 89 (1), 93–122, doi:10.1016/0019-1035(91)90090-G.

Kivelson, M.G., Khurana, K.K., Volwerk, M., 2002. The permanent and inductive magnetic moments of Ganymede. Icarus 157, 507–522, doi:10.1006/icar.2002.6834.

Knittel, K., Lösekann, T., Boetius, A., Kort, R., Amann, R., 2005. Diversity and distribution of methanotrophic archaea at cold seeps. Appl. Environ. Microbiol. 71 (1), 467–479, doi:10.1128/AEM. 71.1.467-479.2005.

Kossacki, K.J., Lorenz, R.D., 1996. Hiding Titan's ocean: Densification and hydrocarbon storage in an icy regolith. Planet. Space Sci. 44 (9), 1029–1037, doi:10.1016/0032-0633(96)00022-0.

Krivchikov, A.I., Gorodilov, B.Ya., Korolyuk, O.A., Manzhelii, V.G., Conrad, H., Press, W., 2005. Thermal conductivity of methane hydrate. J. Low Temp. Phys. 139 (5–6), 693–702, doi:10.1007/s10909-005-5481-z.

Lara, L.M., Lellouch, E., López-Moreno, J.J., Rodrigo, R., 1996. Vertical distribution of Titan's atmospheric neutral constituents. J. Geophys. Res. 101 (E10), 23261–23283, doi:10.1029/96JE02036.

Lara, L.M., Rodrigo, R., Tozzi, G.P., Boehnhardt, H., Leisy, P., 2004. The gas and dust coma of Comet C/1999 H1 (Lee). Astron. Astrophys. 420 (1), 371–382, doi:10.1051/0004-6361:20034214.

Levkam, K., Raj Bishnoi, P., 1997. Dissolution of methane in water at low temperatures and intermediate pressures. Fluid Phase Equilibr. 131, 297–309, doi:10.1016/S0378-3812(96)03229-3.

Lewis, J.S., Prinn, R.G., 1980. Kinetic inhibition of CO and N_2 reduction in the solar nebula. Astrophys. J. 238, 357–364, doi:10.1086/157992.

Lide, D.R. (Ed.), 2005. CRC Handbook of Chemistry and Physics. 86th ed. CRC Press/Taylor & Francis Group, Boca Raton.

López-Valverde, M.A., Lellouch, E., Coustenis, A., 2005. Carbon monoxide fluorescence from Titan's atmosphere. Icarus 175 (2), 503–521, doi:10.1016/j.icarus.2004.12.015.

Lopes, R.M.C., and 43 colleagues, 2007. Cryovolcanic features on Titan's surface as revealed by the Cassini Titan Radar Mapper. Icarus, doi:10.1016/j.icarus.2006.09.006.

Lorenz, R.D., 1996. Pillow lava on Titan: Expectations and constraints on cryovolcanic processes. Planet. Space Sci. 44 (9), 1021–1028, doi:10.1016/0032-0633(95)00139-5.

Lorenz, R.D., 2002. Thermodynamics of geysers: Application to Titan. Icarus 156 (2), 176–183, doi:10.1006/icar.2001.6779.

Lorenz, R.D., Lunine, J.I., 1996. Erosion on Titan: Past and present. Icarus 122 (1), 79–91, doi:10.1016/icar.1996.0110.

Lorenz, R.D., the Cassini RADAR Team, 2005. Titan's methane monsoon: Evidence of catastrophic hydrology from Cassini RADAR. In: 37th DPS Meeting. Abstract 53.07.

Lorenz, R.D., and 39 colleagues, 2006. The sand seas of Titan: Cassini RADAR observations of longitudinal dunes. Science 312, 724–727, doi:10.1126/science.1123257.

Lunine, J.I., Stevenson, D.J., 1987. Clathrate and ammonia hydrate at high pressure: Application to the origin of methane on Titan. Icarus 70 (1), 61–77, doi:10.1016/0019-1035(87)90075-3.

McCarthy, C., Cooper, R.F., Kirby, S.H., Rieck, K.D., Stern, L.A. Solidification and microstructures of binary ice-I/hydrate eutectic aggregates. Am. Mineral. Submitted for publication.

McCord, T.B., Hansen, G.B., Matson, D.L., Johnson, T.V., Crowley, J.K., Fanale, F.P., Carlson, R.W., Smythe, W.D., Martin, P.D., Hibbitts, C.A., Granahan, J.C., Ocampo, A., the NIMS Team, 1999. Hydrated salt minerals on Europa's surface from the Galileo Near-Infrared Mapping Spectrometer (NIMS) investigation. J. Geophys. Res. 104 (E5), 11827–11851, doi:10.1029/1999JE900005.

McCord, T.B., Hansen, G.B., Hibbitts, C.A., 2001. Hydrated salts on Ganymede's surface: Evidence of an ocean below. Science 292, 1523–1525, doi:10.1126/science.1059916.

McKay, C.P., Scattergood, T.W., Pollack, J.B., Borucki, W.J., van Ghyseghem, H.T., 1988. High-temperature shock formation of N_2 and organics on primordial Titan. Nature 332, 520–522, doi:10.1038/332520a0.

McKinnon, W.B., Zolensky, M.E., 2003. Sulfate content of Europa's ocean and shell: Evolutionary considerations and some geological and astrobiological implications. Astrobiology 3 (4), 879–897, doi:10.1089/15311073322736150.

Meier, R., Eberhardt, P., Krankowsky, D., Hodges, R.R., 1994. Ammonia in P/Halley. Astron. Astrophys. 287 (1), 268–278.

Mitchell, K.L., Kargel, J.S., Lopes, R.M.C., Lunine, J., Mitri, G., Lorenz, R., Petford, N., Wilson, L., 2006. Eruption of ammonia–water cryomagmas on Titan. 1. Crystallization and cooling during ascent. Lunar Planet. Sci. XXXVII. Abstract 2355.

Mitri, G., Showman, A.P., Lunine, J.I., Lopes, R., 2006. Resurfacing of Titan by ammonia–water cryomagma. Lunar Planet. Sci. XXXVII. Abstract 1994.

Mitri, G., Lunine, J.I., Showman, A.P., 2007. Hydrocarbon lakes on Titan. Icarus, doi:10.1016/j.icaruc.2006.09.004.

Mohammadi, A.H., Anderson, R., Tohidi, B., 2005. Carbon monoxide clathrate hydrates: Equilibrium data and thermodynamic modeling. AIChE J. 51 (10), 2825–2833, doi:10.1002/aic.10526.

Mousis, O., Gautier, D., Bocklée-Morvan, D., 2002. An evolutionary-turbulent model of Saturn's subnebula: Implications for the origin of the atmosphere of Titan. Icarus 156 (1), 162–175, doi:10.1006/icar.2001.6782.

Nielsen, R.B., Bucklin, R.W., 1983. Why not use methanol for hydrate control? Hydrocarb. Process. 62 (4), 71–78.

Niemann, H.B., and 17 colleagues, 2005. The abundances of constituents of Titan's atmosphere from the GCMS instrument on the Huygens probe. Nature 438, 779–784, doi:10.1038/nature04122.

Nixon, P.H. (Ed.), 1987. Mantle Xenoliths. Wiley, Chichester.

Novotný, P., Söhnel, O., 1988. Densities of binary aqueous solutions of 306 inorganic substances. J. Chem. Eng. Data 33 (1), 49–55, doi:10.1021/je00051a019.

Ohmura, R., Shimada, W., Uchida, T., Mori, Y.H., Takeya, S., Nagao, J., Minegawa, H., Ebinuma, T., Narita, H., 2004. Clathrate hydrate crystal growth in liquid water saturated with a hydrate-forming substance: Variations in crystal morphology. Philos. Mag. 84 (1), 1–16, doi:10.1080/14786430310001623542.

Orlando, T.M., McCord, T.B., Grieves, G.A., 2005. The chemical nature of Europa's surface material and the relation to a subsurface ocean. Icarus 177 (2), 528–533, doi:10.1016/j.icarus.2005.05.009.

Osegovic, J.P., Max, M.D., 2005. Compound clathrate hydrate on Titan. J. Geophys. Res. Planets 110 (E8), doi:10.1029/2005JE002435. Article E08004.

O'Sullivan, T.D., Smith, N.O., 1970. The solubility and partial molar volumes of nitrogen and methane in water and aqueous sodium chloride from 50 to 125° and 100 to 600 atm. J. Phys. Chem. 74 (7), 1460–1466, doi:10.1021/j100702a012.

Owen, T.C., 2000. On the origin of Titan's atmosphere. Planet. Space Sci. 48 (7–8), 747–752, doi:10.1016/S0032-0633(00)00040-4.

Paillou, Ph., Crapeau, M., Elachi, C., Wall, S., Encrenaz, P., 2006. Modeling SAR backscattering of bright flows and dark spots on Titan. Lunar Planet. Sci. XXXVII. Abstract 1285.

Paganelli, F., van Zyl, J., Janssen, M.A., Stiles, B., West, R., Lopes, R.M., Stofan, E.R., Callahan, P., Roth, L., Wall, S.D., Farr, T.G., Elachi, C., Lorenz, R., Soderblom, L., the Cassini Radar Team, 2006. Titan electromagnetic response and surface roughness imaged by the Cassini Radar. Planet. Space Sci. XXXVII. Abstract 1501.

Parfitt, E., 2004. A discussion of the mechanisms of explosive basaltic eruptions. J. Volcanol. Geoth. Res. 134, 77–107, doi:10.1016/j.jvolgeores.2004.01.002.

Pawley, A.R., Clark, S.M., Chinnery, N.J., 2002. Equation of state measurements of chlorite, pyrophyllite, and talc. Am. Mineral. 87, 1172–1182.

Perovich, D.K., Gow, A.J., 1996. A quantitative description of sea ice inclusions. J. Geophys. Res. 101 (C8), 18327–18343, doi:10.1029/96JC01688.

Pieri, D.C., Baloga, S.M., 1984. Effusion rates, areas and lengths for some lava flows on Hawaii and Mt. Etna with planetary implications. Rept. Planet. Geol. Geophys. Program-1983. NASA TM-86246.

Pinkerton, H., Wilson, L., Macdonald, R., 2002. The transport and eruption of magma from volcanoes: A review. Contemp. Phys. 43 (3), 197–210, doi:10.1080/00107510110097756.

Porco, C.C., West, R.A., Squyres, S., Mcewen, A., Thomas, P., Murray, C.D., Delgenio, A., Ingersoll, A.P., Johnson, T.V., Neukum, G., Veverka, J., Dones, L., Brahic, A., Burns, J.A., Haemmerle, V., Knowles, B., Dawson, D., Roatsch, T., Beurle, K., Owen, W., 2004. Cassini imaging science: Instrument characteristics and anticipated scientific investigations at Saturn. Space Sci. Rev. 115, 363–497, doi:10.1007/s11214-004-1456-7.

Prentice, A.J.R., 1984. Formation of the saturnian system: A modern Laplacian theory. Earth Moon Planets 30 (3), 209–228, doi:10.1007/BF00056200.

Prieto-Ballesteros, O., Kargel, J.S., 2006. Clathration as a process for the cryomagmatic differentiation of icy satellites: Application to Enceladus and Europa. Lunar Planet. Sci. XXXVII. Abstract 1971.

Prinn, R.G., Fegley Jr., B., 1981. Kinetic inhibition of CO and N_2 reduction in circumplanetary nebulae: Implications for satellite composition. Astrophys. J. 249, 308–317, doi:10.1086/159289.

Radebaugh, J., Lorenz, R., Kirk, R., Lunine, J., 2006. Mountains on Titan observed by Cassini RADAR. Lunar Planet. Sci. XXXVII. Abstract 1007.

Rappaport, N., Bertotti, B., Giampieri, G., Anderson, J.D., 1997. Doppler measurements of the quadrupole moments of Titan. Icarus 126 (2), 313–323, doi:10.1016/icar.1996.5661.

Rehder, G., Brewer, P.W., Peltzer, E.T., Friederich, G., 2002. Enhanced lifetime of methane bubble streams within the deep ocean. Geophys. Res. Lett. 29 (15), doi:10.1029/2001GL013966. Article 1731.

Roe, H.G., Brown, M.E., Schaller, E.L., Bouchez, A.H., Trujillo, C.A., 2005. Geographic control of Titan's mid-latitude clouds. Science 310, 477–479, doi:10.1126/science.1116760.

Ruffle, D.P., Herbst, E., 2000. New models of interstellar gas-grain chemistry. I. Surface diffusion rates. Mon. Not. R. Astron. Soc. 319 (3), 837–850, doi:10.1046/j.1365-8711.2000.03911-x.

Salisbury, J.W., D'Aria, D.M., Wald, A., 1994. Measurement of the thermal infrared spectral reflectance of frost, ice, and snow. J. Geophys. Res. 99 (B12), 24235–24240, doi:10.1029/94JB00579.

Sauter, E.J., Muyakshin, S.I., Charlou, J.-L., Schlüter, M., Boetius, A., Jerosch, K., Damm, E., Foucher, J.-P., Klages, M., 2006. Methane discharge from a deep-sea submarine mud volcano into the upper water column by gas hydrate-coated methane bubbles. Earth Planet. Sci. Lett. 243, 354–365, doi:10.1016/j.epsl.2006.01.041.

Schaller, E.L., Brown, M.E., Roe, H.G., Bouchez, A.H., 2006. A large cloud outburst at Titan's south pole. Icarus 182 (1), 224–229.

Schenk, P., Jackson, M.P.A., 1993. Diapirism on Triton: A record of crustal layering and instability. Geology 21 (4), 299–302, doi:10.1130/0091-7613(1993)021<0299:DOTARO>2.3.CO.

Schutte, C.J.H., Heyns, A.M., 1970. Low-temperature studies. IV. The phase transitions of ammonium sulfate and ammonium-d4 sulfate; the nature hydrogen bonding and the reorientation of the NX^{4+} ions. J. Chem. Phys. 52 (2), 864–871, doi:10.1063/1.1673066.

Scott, H.P., Williams, Q., Ryerson, F.J., 2002. Experimental constraints on the chemical evolution of large icy satellites. Earth Planet. Sci. Lett. 203 (1), 399–412, doi:10.1016/S0012-821X(02)00850-6.

Sekine, Y., Sugita, S., Shido, T., Yamamoto, T., Iwasara, Y., Kadono, T., Matsui, T., 2005. The role of Fischer–Tropsch catalysis in the origin of methane-rich Titan. Icarus 178 (1), 154–164, doi:10.1016/j.icarus.2005.03.016.

Showman, A.P., Mosqueira, I., Head III, J.W., 2004. On the resurfacing of Ganymede by liquid-water volcanism. Icarus 172 (2), 625–640, doi:10.1016/j.icarus.2004.07.011.

Sloan, E.D., 1990. Clathrate Hydrates of Natural Gases. Dekker, New York.

Sohl, F., Hussmann, H., Scwentker, B., Spohn, T., Lorenz, R.D., 2003. Interior structure models and tidal Love numbers of Titan. J. Geophys. Res. 108 (E12), doi:10.1029/2003JE002044. Article 5130.

Sohl, F., Sears, W.D., Lorenz, R.D., 1995. Tidal dissipation on Titan. Icarus 115 (2), 278–294, doi:10.1016/icar.1995.1097.

Spaun, N.A., Head III, J.W., 2001. A model of Europa's crustal structure: Recent Galileo results and implications for an ocean. J. Geophys. Res. 106 (E4), 7567–7576, doi:10.1029/2000JE001270.

Spencer, J.R., Grundy, W.M., Dumas, C., Carlson, R.W., McCord, T.B., Hansen, G.B., Terrile, R.J., 2006. The nature of Europa's dark non-ice surface material: Spatially resolved high spectral resolution spectroscopy from the Keck telescope. Icarus 182, 202–210, doi:10.1016/j.icarus.2005.12.024.

Sprung, A., 1876. 1. Experimentelle Untersuchungen über die Flüssigkeitsreibung bei Salzlösungen. Ann. Phys. Chem. 159 (9), 1–35. http://gallica.bnf.fr/ark:/12148/bpt6k152436.

Takeya, S., Ebinuma, T., Uchida, T., Nagao, J., Narita, H., 2002. Self-preservation effect and dissociation rates of CH_4 hydrate. J. Cryst. Growth 237–239 (1), 379–382, doi:10.1016/S0022-0248(01)01946-7.

Thompson, W.R., Squyres, S.W., 1990. Titan and other icy satellites: Dielectric properties of constituent materials and implications for radar sounding. Icarus 86, 336–354.

Tobie, G., Lunine, J.I., Sotin, C., 2006. Episodic outgassing as the origin of atmospheric methane on Titan. Nature 440, 61–64, doi:10.1038/nature04497.

Tobie, G., Grasset, O., Lunine, J.I., Mocquet, A., Sotin, C., 2005. Titan's internal structure inferred from a coupled thermal-orbital model. Icarus 175 (2), 496–502, doi:10.1016/j.icarus.2004.12.007.

Tomasko, M.G., Buchhauser, D., Bushroe, M., Dafoe, L.E., Doose, L.R., Eibl, A., Fellows, C., Farlane, E.M., Prout, G.M., Pringle, M.J., Rizk, B., See, C., Smith, P.H., Tsetsenekos, K., 2002. The Descent Imager/Spectral Radiometer (DISR) experiment on the Huygens entry probe of Titan. Space Sci. Rev. 104 (1), 469–551, doi:10.1023/A:1023632422098.

Tomasko, M.G., and 39 colleagues, 2005. Rain, winds and haze during the Huygens probe's descent to Titan's surface. Nature 438, 765–778, doi:10.1038/nature04126.

Torres, M.E., Wallmann, K., Tréhu, A.M., Bohrmann, G., Borowski, W.S., Tomaru, H., 2004. Gas hydrate growth, methane transport, and chloride enrichment at the southern summit of Hydrate Ridge, Cascadia margin off Oregon. Earth Planet. Sci. Lett. 226, 225–241, doi:10.1016/j.epsl.2004.07.029.

Ussler, W., Paull, C.K., 2001. Ion exclusion associated with marine gas hydrate deposits. In: Dillon, W.P., Paull, C.K. (Eds.), Natural Gas Hydrates—Occurrence, Distribution and Detection. American Geophysical Union, pp. 41–51.

Waite, J.H., Combi, M.R., Ip, W.-H., Cravens, T.E., McNutt Jr., R.L., Kasprzak, W., Yelle, R., Luhmann, J., Niemann, H., Gell, D., Magee, B., Fletcher, G., Lunine, J., Tseng, W.-L., 2006. Cassini Ion and Neutral Mass Spectrometer: Enceladus plume composition and structure. Science 311, 1419–1422, doi:10.1126/science.1121290.

Wood, C.A., Lunine, J.I., Lopes, R.M., Stofan, E.R., Mitchell, K., Radebaugh, J., 2006. Crateriform structures on Titan. Lunar Planet. Sci. XXXVII. Abstract 1659.

Wunder, B., Schreyer, W., 1997. Antigorite: High-pressure stability in the system $MgO–SiO_2–H_2O$ (MSH). Lithos 41 (1–3), 213–227, doi:10.1016/S0024-4937(97)82013-0.

Wye, L., Zebker, H., Lorenz, R., the Cassini RADAR Team, 2006. Modeling Titan's surface from Cassini RADAR's scatterometer and radiometer measurements. Lunar Planet. Sci. XXXVII. Abstract 1473.

Xu, J., Imre, D., McGraw, R., Tang, I., 1998. Ammonium sulfate: Equilibrium and metastability phase diagrams from 40 to −50 °C. J. Phys. Chem. B 102 (38), 7462–7469, doi:10.1021/jp981929x.

Zahnle, R., Pollack, J.P., Grinspoon, D., Done, L., 1992. Impact generated atmospheres over Titan, Ganymede, and Callisto. Icarus 95 (1), 1–23, doi:10.1016/0019-1035(92)90187-C.

Zimmer, C., Khurana, K.K., Kivelson, M.G., 2000. Subsurface oceans on Europa and Callisto: Constraints from Galileo magnetometer observations. Icarus 147, 329–347, doi:10.1006/icar.2000.6456.

Zolotov, M.Y., Shock, E.L., 2001. Composition and stability of salts on the surface of Europa and their oceanic origin. J. Geophys. Res. 106 (E12), 32815–32827, doi:10.1029/2000JE001413.

Zolotov, M.Y., Shock, E.L., 2003. Energy for biologic sulfate reduction in a hydrothermally formed ocean on Europa. J. Geophys. Res. 108 (E4), doi:10.1029/2002JE001966. Article 5022.

Zolotov, M.Y., Owen, T., Atreya, S., Niemann, H.B., Shock, E.L., 2005. An endogenic origin of Titan's methane. In: American Geophysical Union Fall Meeting 2005. Abstract P43B-04.